JOTCS A
Journal of the Turkish Chemical Society
Section: A
Chemistry
TURKISH CHEMICAL SOCIETY

Li^+ doped chitosan-based solid polymer electrolyte incorporated with PEDOT:PSS for electrochromic device

Esin EREN[1,2*]

[1] University of Suleyman Demirel, Innovative Technologies Application and Research Center, 32260, Isparta, Turkey.
[2] University of Suleyman Demirel, Faculty of Arts and Science, Department of Chemistry, 32260 Isparta, Turkey.

Abstract: In this study, solid polymer electrolyte-based on chitosan was prepared with addition of PEDOT:PSS, lithium trifluoromethane sulfonate, propylene carbonate by solvent casting technique. The chitosan-based polymer electrolytes without PEDOT:PSS, with PEDOT:PSS were characterized using electrochemical impedance spectroscopy. The ionic conductivity value was calculated as 4.2 x 10^{-4} S/cm for the chitosan-based electrolyte including PEDOT:PSS. The SPE having good ionic conductivity was used to fabricate electrochromic device with glass/ITO/WO_3|PEDOT:PSS-Ch-LiTRIF-PC|ITO/glass whose performance was evaluated via cyclic voltammetry, transmittance, and repeating chronoamperometry. The optical contrast of ECD was attained as 22% at 800 nm, resulting in a coloration efficiency of 67 cm^2/C. The ECD displays fast response time for coloration (t_c), which is 0.29 s. Upon reversal of potential bleaching (t_b) forms within 3 s. The findings demonstrated that this SPE electrolyte has promising candidate for use in optoelectronic applications.

Keywords: Chitosan, Electrolyte, Electrochromic Device, PEDOT:PSS.

Submitted: June 14, 2018. **Accepted:** December 27, 2018.

Cite this: Eren E. Li+ doped chitosan-based solid polymer electrolyte incorporated with PEDOT:PSS for electrochromic device. JOTCSA. 2018;5(3):1413-22.

DOI: http://dx.doi.org/10.18596/jotcsa.433901.

***Corresponding author. E-mails:** eso_eren@yahoo.com.tr, esineren@sdu.edu.tr.

INTRODUCTION

SPEs have gained great interest due to their potential applications like sensors, photovoltaic cells, electrochromic devices, and smart electronics (1). An ECD acts as a thin film battery that alters optical features after application of an electric input (2, 3). In general, a conventional ECD includes five electroactive layers, an ion conducting electrolyte sandwiched via an electrochromic (EC) layer and ion-storage layer that are individually deposited on transparent conductive substrates (4). Ion conducting electrolyte supplies the ionic conduction layer between the electrochromic layer and the ion-storage layer (5). Nowadays, these devices are of great attention to technological and commercial applications, explaining why diverse SPEs have been suggested for this aim (6). WO_3 is a very encouraging cathodic electrochromic compound, which has superior electrochromic characteristics such as optical contrast and stability. Thus, it is one of widely used as an electrochromic material (2, 7).

Biodegradable polymers such as polyethylene oxide and chitosan are commonly used, and further scientific research using SPE system are in progress (8). SPEs supply the advantages of compactness and reliability without the leakage of liquid components (8). Chitosan (Ch) is a type of cationic amino-polysaccharide that is acquired from the alkaline deacetylation of chitin (8). Its chemical structure consists of reactive amino and hydroxyl groups which feature own lone pair electrons that are appropriate to produce solid polymer electrolytes (9, 10). Due to the existence of polar functional groups along its chain, chitosan can also solvate inorganic salts and show the features adherent to polymer electrolytes (11,

12). The presence of lone pair electrons allows the chelation of a proton donor supplied by a salt (13, 14). However, chitosan-based films can display low ionic conductivity. At low pH, the primary amines get protonated to have positive charges and leave the hydroxyl groups free that produces chitosan a water-soluble cationic polyelectrolyte. This may promote ionic conduction (15, 16). One way to obtain enhanced ionic conductivity is to add plasticizers in polymer electrolytes which can be preferred due to the creation of free volume. Furthermore, ionic conductivity can be ascribed to the amorphous phase. Dissolution of salts (such lithium salts) in the polymer matrix is one of the several used approaches to acquire amorphous phase (1). Alves *et al.* fabricated ECD with WO_3/Chitosan$_{33.32}$Ce$(CF_3SO_3)_3$/CeO_2–TiO_2 configuration which displayed an alteration from transparent to blue color with 5% of percent transmittance change at 633 nm (17). Two years later, new SPEs of chitosan complexed with $Sm(CF_3SO_3)_3$ including glycerol were prepared for solid state electrochromic devices. The changes of transmittance of ECD with WO_3 electrochromic layer are measured as 4.1%, 4.6% at 550 nm, 633 nm, respectively (6). Herein, this study demonstrated that ECD including the biohybrid electrolyte system with PEDOT:PSS exhibited improved electrochromic characteristics, especially enhanced optical contrast, when compared to those of ECD composed of chitosan-based electrolyte systems (6, 17).

PEDOT:PSS is one of the most used electronically conducting polymers due to its robust mechanical properties, good film forming ability, and high electrical conductivity (18, 19). Zhang *et al.* prepared a novel kind of biocompatible micelles including PEDOT:PSS and chitosan for electrochemical biosensor (19). Due to the good electrostatic interaction between chitosan and PEDOT:PSS, PEDOT:PSS can be used to prepare chitosan-based SPEs (19).

The main propose of this paper is to provide a significant contribution on the chitosan-based solid polymer electrolyte with the addition of PEDOT:PSS in terms of electrochromic applications. The chitosan-based SPE consisting of acetic acid, LiTRIF and PEDOT:PSS was plasticized with PC. For this purpose, a biohybrid electrolyte-based ECD with glass/ITO/WO_3|PEDOT:PSS-Ch-LiTRIF-PC|ITO/glass was fabricated and analyzed using electrochemical, transmittance measurements. To the best of my knowledge, the WO_3-based ECD consisting of the chitosan-based electrolyte system with the addition of PEDOT:PSS has hitherto been unexplored for electrochromic applications.

EXPERIMENTAL

Materials

W nanopowder was supplied by SkySpring Nanomaterials. Chitosan with medium molecular weight (1.10×10^6 g/mol (DD:75–85)), PEDOT:PSS were purchased from Sigma-Aldrich. LiTRIF from Sigma-Aldrich, PC from Sigma-Aldrich, DMSO from Sigma-Aldrich, and acetic acid from Merck were used as received. ITO-coated glass sheets were purchased from Plazmatek A.Ş. Company/Turkey and were cleaned with ethanol and deionized water prior to use.

Preparation of the WO_3 Film

The WO_3 sol was prepared by dissolving W powder into 30% H_2O_2 and adding ethanol and water. The electrodeposition was performed using a three-electrode electrochemical system with a platinum wire as the counter electrode, Ag/AgCl as the reference electrode and ITO coated glass as the working electrode at room temperature. Deposition was carried out by applying a constant voltage (-0.45 V) for 15 min. Then, the prepared thin film was rinsed with distilled water and dried in air.

The mechanism of the electrodeposition of WO_3 can be explained via the two-stage reaction processes (20):

$$2W + 10H_2O_2 \rightarrow W_2O_{11}^{2-} + 2H^+ + 9H_2O \quad \text{(Eq. 1)}$$

$$W_2O_{11}^{2-} + (2+n)H^+ + ne^- \rightarrow 2WO_3 + (2+n)/2H_2O + (8-n)/4O_2 \quad \text{(Eq. 2)}$$

Preparation of the SPE

The solution casting method was used for the preparation of chitosan-based SPE. 0.2 g of chitosan powder was dissolved in 10 mL of 2% acetic acid solution. The mixture was stirred continuously for one day to complete dissolution. Then, 1.2 g of LiTRIF and 4 g of PC as plasticizer were added into this solution under stirring at room temperature. The resulting solution was stirred for one day until homogeneous dispersion. PEDOT:PSS solution was doped with 5 wt% DMSO. The resulting PEDOT:PSS solution was then added 2.5 w% with respect to the weight of all other components. Continuous stirring for two days was conducted to ensure complete dissolution.

Construction of the ECD

The prepared viscous electrolyte was poured on ITO-coated glass sheets and dried at room temperature to form transparent SPE. The actual pixel electrode dimension was described as 1.3 cm^2 using double-sided adhesive foam band. The ECD was fabricated by sandwiching of SPE including chitosan and PEDOT:PSS between working (WO_3) and counter (ITO coated glass) electrodes. The schematic illustration of the electrochromic structure device is shown in Figure 1.

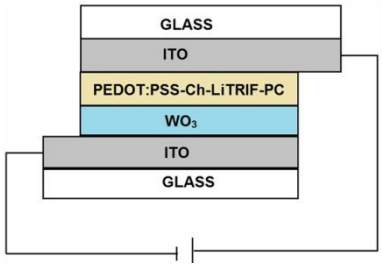

Figure 1. Schematic illustration of the electrochromic structure device

Characterization

Electrochemical properties were evaluated using a Gamry PCI4/300 model potentiostat/galvanostat. Electrochromic studies were performed using a standard three-electrode system, electrochromic film as working electrode, a Pt wire as counter electrode and a Ag/AgCl with 3 M KCl as reference electrode were used. Optical transmittance of solid-state ECD was attained using a computer-controlled setup of HR4000 (Ocean Optics, Dunedin, FL, USA) in the wavelength range of 400-900 nm. The surface morphology and composition analysis of the WO_3 film were performed using a SEM-EDS with the brand FEI Quanta FEG 250. EIS measurements were performed in the frequency range of 0.1 Hz-10 kHz by use of an AC voltage amplitude (10 mV), and CHI760E electrochemical workstation.

RESULTS AND DISCUSSION

SEM result of the WO_3 films

Figure 2 displays the SEM image of the electrodeposition of WO_3 thin film. SEM observation has shown a nano-grain formation with the close-packed structure. The WO_3 film is uniform and dense. The chemical composition of the electrodeposited WO_3 thin film was evaluated using EDS spectrum (Figure 3). The elemental composition of the WO_3 film with its at% and wt% are shown as the inset. The table demonstrates the existence of W and O. The element W is from WO_3, Sn and In are from ITO substrate, and O is from both WO_3 and ITO substrate. The absence of any other peaks except ITO substrate due to W and O confirms the deposition of WO_3 film without any elemental impurities.

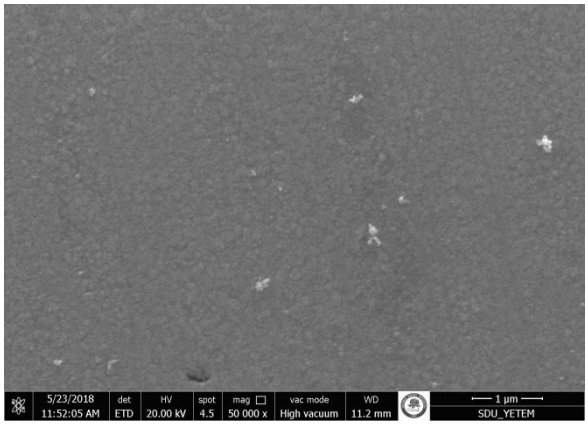

Figure 2. SEM images of WO_3 film onto ITO coated glass at 50000X magnification.

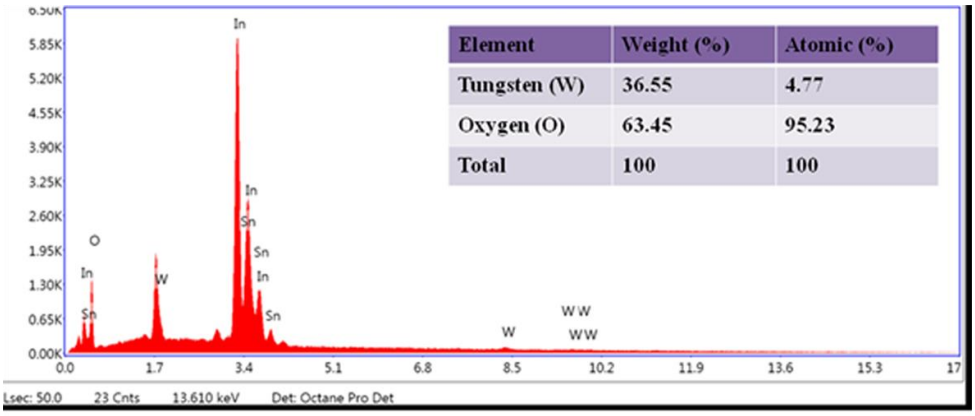

Element	Weight (%)	Atomic (%)
Tungsten (W)	36.55	4.77
Oxygen (O)	63.45	95.23
Total	100	100

Figure 3. EDS spectrum of WO_3 film onto ITO coated glass.

Ionic Conductivity Result of SPE

The electrolyte plays a significant role in the ECD, and is used to conduct ions between the electrochromic layer and the ion-storage layer (21). One of the main criteria for applications in various electrochemical devices is to attain high ionic conductivity of electrolytes (22). Most of the electrochromic devices need to have $>10^{-4}$ Scm^{-1} of ionic conductivity to allow effective performance (23). Ionic conductivities of the prepared solid polymer electrolyte with PEDOT:PSS and without PEDOT:PSS were measured via electrochemical impedance spectroscopy (EIS). EIS was operated with 'ITO

coated glass/electrolyte/ITO coated glass' structure at a constant potential of +0.1 V in the frequency range of 0.1 Hz-10 kHz at room temperature. In this work, the low potential (0.1 V) was used because 0.1 V potential allows to prevent from additional effect of electrode polarization on occurrence of complicated ion layers on the electrode surface (24). Figure 4 shows the Nyquist plot of chitosan-based solid polymer electrolytes with PEDOT:PSS, without PEDOT:PSS. The ionic conductivity (σ) was calculated using equation 3 (25, 26):

$$\sigma = \frac{L}{R_b * A} \qquad \text{(Eq. 3)}$$

where σ is the ionic conductivity, L is the distance between the two electrodes, R_b is the bulk resistance of the SPE, and A is the area of the sample (1 cm^2). R_b (bulk resistance) value of the solid electrolyte can be obtained from the intercept with the Z'-axis (27-30). The ionic conductivities of the chitosan-based electrolyte without PEDOT:PSS and with PEDOT:PSS solution were calculated as 3.40 x 10^{-4}, 4.2 x 10^{-4} S/cm, respectively. The decrease of R_b leads to the enhanced ionic conductivity after introduction of PEDOT:PSS in chitosan-based electrolyte, as seen in Figure 4. Ionic conductivity plays one of significant roles for availability of the mobility of ions during the electrochromic switching procedure. Enhancement in ionic conductivity can lead to rapid switching time (31). Similar results were acquired for electrolytes based on other polysaccharides (32, 33). For example, Andrade *et al.* prepared plasticized pectin-based gel electrolytes with 68 wt.% of glycerol that showed an ionic conductivity of 4.7 x 10^{-4} S/cm (32). Alves *et al*. prepared a type of erbium triflate doped chitosan electrolytes using solvent casting method. The highest ionic conductivity values were calculated as 2.06 x 10^{-5} and 5.91 x 10^{-4} Scm^{-1} at 30 °C, 90 °C, for electrolytes including higher amount of glycerol, respectively (1).

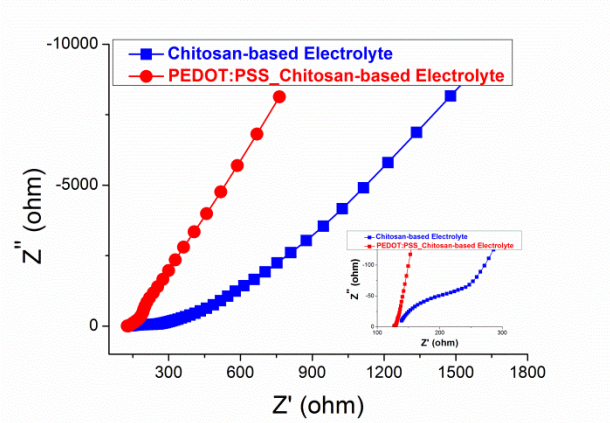

Figure 4. Nyquist diagrams corresponding to chitosan-based electrolyte with PEDOT:PSS and without PEDOT:PSS.

Performance of the ECDs

Figure 5 displays *in situ* transmittance responses at 800 nm of ECD with potential being switched between +3 V and -3 V for 30 s per step. Electrochromic switching of ECD was evaluated by probing the transmittance modulations under a square-wave potential step. The response time was controlled by stepping the potential repeatedly between coloration and bleaching states. The transmittance change was analyzed as a function of time at a certain wavelength. For WO_3-based ECD, the voltage was stepwise switched between +3 V and -3 V at 800 nm via applying a square-wave potential step of 30 s with 3 cycles. The coloration and bleaching times are described as the time required for a 90 % change in the whole transmittance modulation at 800 nm (34). The optical contrast (ΔT) for this ECD was found as 22% with the switching time of 0.29 s for coloring step and 3 s for bleaching step. Rocha *et al.* prepared an ECD with configuration ITO/NiO/$LiClO_4$-PC-PMMA/WO_3/ITO that had optical contrast values ranging from 8% to 28% (35). As reported by Ling *et al.*, the hybrid electrochromic films consisting of WO_3 nanoparticles, PEDOT: PSS and PEI showed the optical contrast of 20% at the wavelength of around 633 nm (36). Aiming to figure out the reversibility of WO_3-based ECD with chitosan electrolyte incorporating PEDOT:PSS, the ECD was subjected to CA cycling by application of different electric potentials (-3 V , +3 V) with a time step of 30 s for 3 cycles (Figure 5b). The decrease in current density as a function of time is due to the enhanced chemical potential of the injected cations (Li^+) as intercalation steps (18, 37). As seen from Figure 5, there is no significant change of transmittance percent or current density during repetitive cycle, indicating superior stability and reversibility of ECD. The ECD displays response time for coloration (t_c) is 0.29 s. Upon reversal of potential rapid bleaching (t_b) forms within 3 s. As published by Chang-Jian *et al.*, WO_3/PEDOT:PSS-based ECD incorporated with TEMPO and $LiClO_4$ reveals a response time of 1.1 s (38). ECD was prepared using $PProDOTMe_2$ as the working electrode, Li-Ti-NiO as the counter electrode. The ECD with polyvinyl butyral and polyethylene glycol-based hybrid QSPEs attain a fast response between colored and bleached state

(t_c=1.2 s, t_b=2.6) (4). Liu *et al*. incorporated carbon nanotubes and chitosan into WO_3 films, resulting in the optical modulation of 13.5%, rapid coloration (t_c=1.9 s) and bleaching times (t_b=1.0 s) (34). In this study, the obtained optical contrast and response times for ECD were comparable with literature (4,34,38). The calculated switching times of ECD were faster than 4 s, which contributes for requirements of electrochemical devices (0.1-10s) (39).

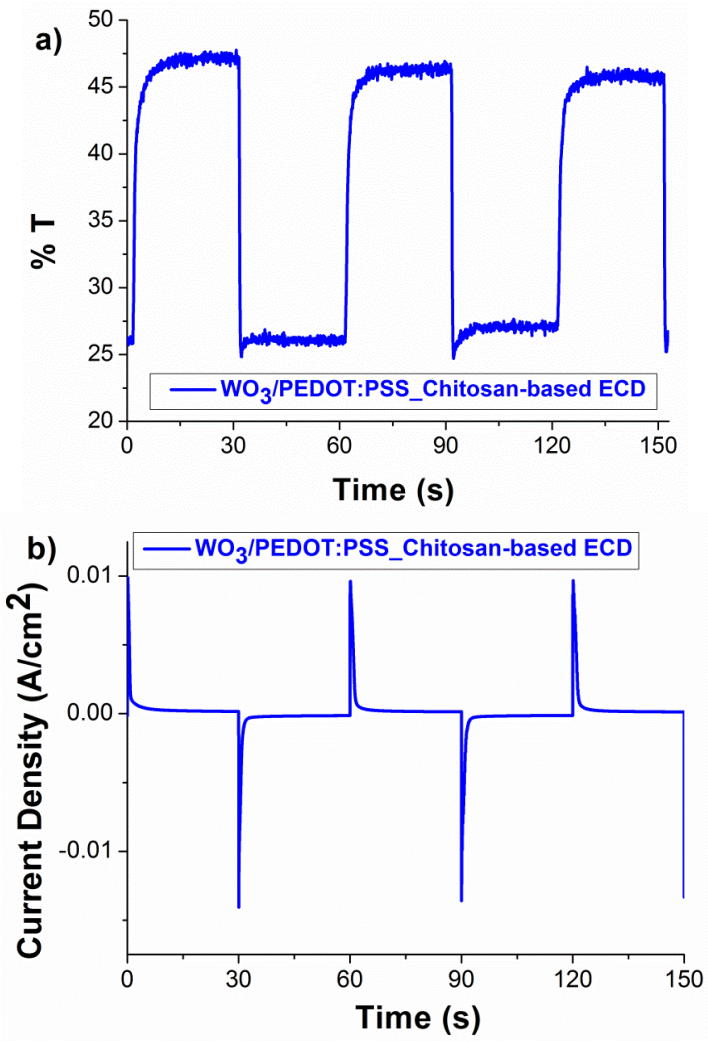

Figure 5. a) Transmittance and b) current density change of electrochromic devices based on WO_3/PEDOT:PSS_Chitosan for applied potentials of ±3 V (monitored at 800 nm).

The colored and bleached states of ECD are displayed in Figure 6. Upon the applied voltage of -3 V, Li^+ ions insert into the PEDOT:PSS layer with the charge balancing counter flow of electrons through the external circuit to compensate for the negative charges of the SO_3^- groups on the PSS polyanion which leads to reduction of PEDOT:PSS layer. The Li^+ ions permeate down to the WO_3 layer with the counter electrons which causes the reduction from W^{6+} ions to W^{5+} ions. The above mentioned processes induces to an alternation in the electron density in the ECD changing the color from light blue to dark blue color. On the other hand, when the applied potential is increased to the positive potential (+3 V), the deintercalations of the Li^+ ions and electrons take place, and the bleached state occurred as a result of the oxidation procedure (40). The electrochemical behavior of WO_3 and PEDOT:PSS accompanies the following electrochemical reaction (2, 41, 42):

$$\boldsymbol{WO_3 + xLi^+ + xe^- \leftrightarrow Li_xWO_3}$$

(colorless, oxidized) (deep blue, reduced) (Eq. 4)

$$\boldsymbol{PEDOT^+PSS^- + Li^+ + e^- \leftrightarrow PEDOT^0 + PSS^-Li^+}$$

(light blue, oxidized) (dark blue, reduced) (Eq. 5)

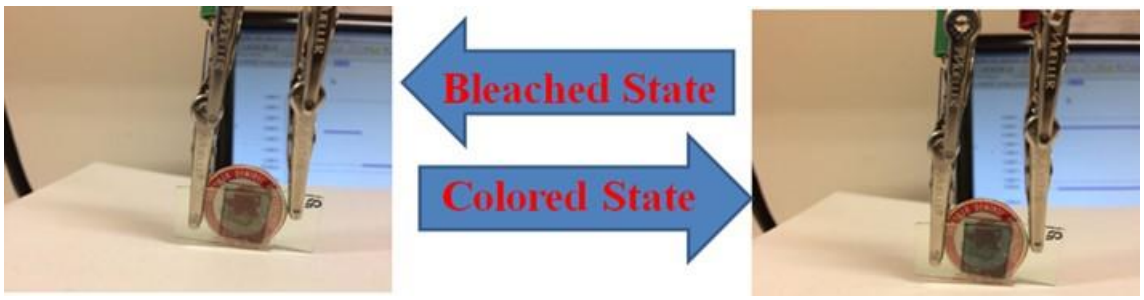

Figure 6. Photographs of the electrochromic device (ECD) based on WO_3/PEDOT:PSS_Chitosan in the two extreme states (a) in its bleached state at + 3 V (b) in its colored state at - 3 V.

Typical cyclic voltammograms of this ECD, recorded during the 1st, 10th, and 20th cycles at 50 mVs^{-1}, are shown in Figure 7. According to the CV scan results in Figure 7, the application of an increasingly negative voltage to the ECD in the dark blue color state brings about an enhanced cathodic current due to the reduction of WO_3, and it is accompanied via a simultaneous alteration to bleached state (43). A large anodic peak has its maximum centered at 0.79 V. Moreover, the broad voltammetric wave was seen during both anodic and cathodic processes. It can belong to overlapping of WO_3 and PEDOT:PSS redox peaks (33). After the 20th cycle, cyclic voltammetric studies also showed a nice electrochemically reversible behavior with a little loss of current density, however.

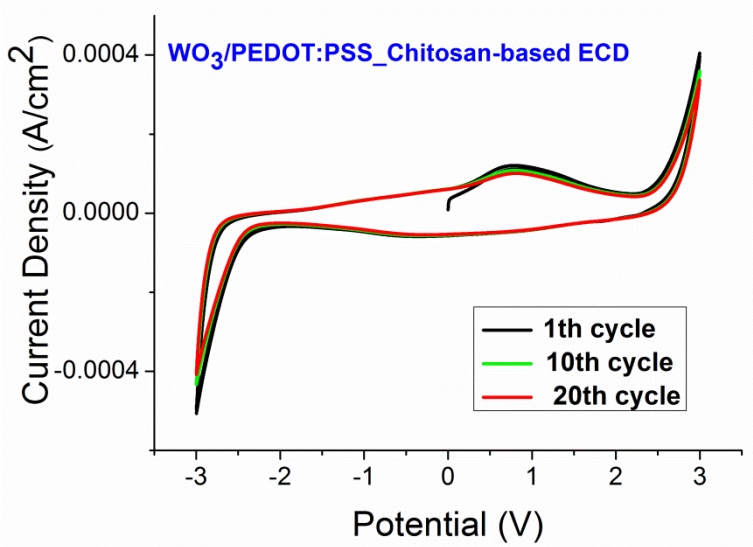

Figure 7. Cyclic voltammograms of electrochromic device (ECD) based on WO_3/PEDOT:PSS_Chitosan during 20 cycles.

CVs were carried out for ECDs with linear potential sweep between -3.0 V and +3.0 V at various scan rates ranging from 25 to 200 mV/s^{-1} (Figure 8a). The area of CVs possesses a direct associated with the amount of charge involved in the intercalation process. The electrochemical characteristics shift to higher value with the increase of the scan rate (Figure 8b). The perfect linear relationship indicated that the redox process of the electroactive film is controlled by the ion from the electrolyte to the electrode surface and redox processes were reversible in all cases even at elevated scan rates (2, 44).

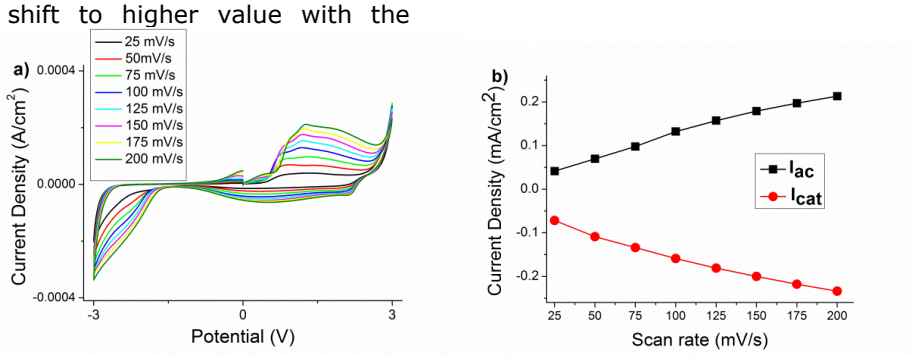

Figure 8. CVs of the ECD at different scan rates (a) plot of cathodic/anodic current density versus scan rate where I_{ac} and I_{cat} denote the anodic and cathodic peak current density, respectively (b).

Chronocoulometric (CC) measurement was performed for WO_3/PEDOT:PSS_Chitosan- based ECD at ±3 V for a step of 30 s to evaluate the alternation in their charge density of Li^+ during the intercalation and deintercalation process as a function of time (Figure 9). The percent electrochromic reversibility of ECD was calculated using Equation 6 (2, 45):

$$Reversibility\ (\%) = \frac{Q_{di}}{Q_i} \times 100 \qquad \text{(Eq. 6)}$$

where Q_i and Q_{di} are the amount of charge intercalated and deintercalated in the electrode, respectively. The reversibility was calculated as 82.19% for WO_3/PEDOT:PSS_Chitosan-based ECD.

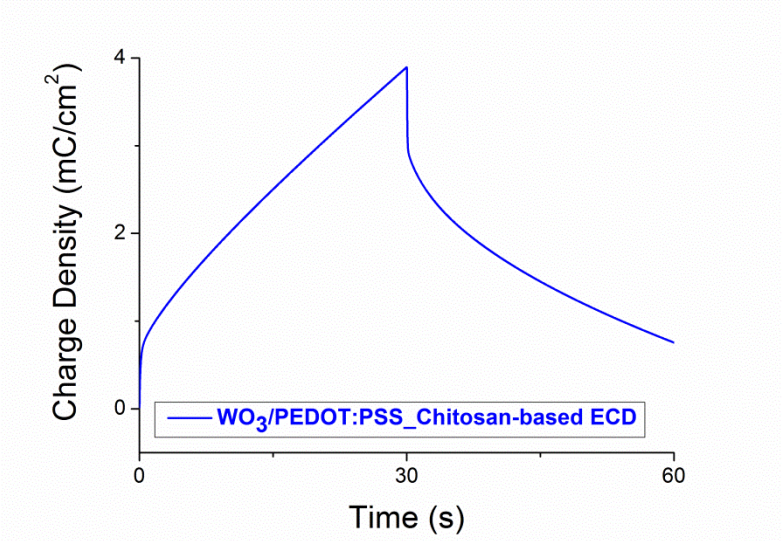

Figure 9. Chronocoulometric study for WO_3/PEDOT:PSS_Chitosan- based ECD.

Coloration efficiency (CE) is a critical factor to evaluate the power consumption of an ECD since it signifies the alteration in optical density at the monitoring wavelength per inserted (extracted) charge (46). In general, the CE value can be calculated using the following equations (2, 44).

$$\Delta OD = log(\frac{T_b}{T_c}) \qquad \text{(Eq. 7)}$$

$$CE = \frac{\Delta OD}{Q_d} \qquad \text{(Eq. 8)}$$

where T_b and T_c represent the transmittances of the ECD in the bleached and colored states at a specific wavelength, respectively. ΔOD is the change in optical density, which is proportional to the amount of formed color centers. Q_d is the charge density inserted (extracted). CE was calculated as 67 cm^2/C. Bathe *et al.* investigated the electrochromic features of fibrous reticulated WO_3 films fabricated from ammonium tungstate precursor using a pulsed spray. The electrochromic optical contrast and coloration efficiency were found to be ~12%, 34 cm^2/C, respectively (47). The electrochromic device with the configuration ITO/WO_3-PEDOT/ACN:PC:PMMA:$LiClO_4$ gel electrolyte/ ITO has a CE of 41.61 cm^2/C (48). In another study, the coloration efficiency of WO_3-based ECD with Li^+ and Er^{3+} doped poly(ε-caprolactone)/siloxane biohybrid electrolytes was calculated as 10.8 cm^2/C (49). In this study, the calculated CE value of ECD is better than those several reported earlier (47-49). Electrochromic performance comparison of this work and several reported works based on electrochromic applications are presented in Table 1. In this study, the ECD obviously shows a higher value in optical contrast when compared to chitosan-based ECDs (6,17). Moreover, the response times is still faster than those in previous reports which utilized WO_3 as electrochromic material (36, 50). As a result, the electrochromic performance is higher than the several published articles based on electrochromic applications (6,17,36, 50, 51).

Table 1. Electrochromic performance comparison of this work and several published work on electrochromic applications

Sample	Electrolyte	Δ%T	t_c (s)	t_b (s)	CE (cm^2/C)	References
WO_3	Chitosan/LiTRIF/ PEDOT:PSS	22	0.29	3	67	This work
WO_3	**PMMA/$LiClO_4$**	**20.17**	**21.4**	**18.5**	**76.82**	**50**
PEDOT:PSS	PEO:$LiClO_4$	28	10	1	377	51
WO_3/ PEDOT:PSS/PEI	**$LiClO_4$**	**20**	**8**	**-**	**117.7**	**36**
WO_3/CeO_2-TiO_2	Chitosan-$Ce(CF_3SO_3)_3$	5	-	-	-	17
WO_3/CeO_2-TiO_2	**Chitosan/ Samarium (III) triflate**	**4.6**	**-**	**-**	**-**	**6**
Prussian blue (PB)	Chitosan/ Samarium (III) triflate	9.2	-	-	-	6

CONCLUSION

This study elucidates on the fabrication of ionically conducting systems based on Ch as the base polymer matrix, PEDOT:PSS as conductive polymer, LiTRIF as guest salt, and PC as the plasticizer. The fabricated electrolyte including PEDOT:PSS showed an ionic conductivity value of 4.2×10^{-4} S/cm. ECD in ITO/WO_3|PEDOT:PSS-Ch-PC|ITO was assembled. The performance of the electrochromic device was analyzed via CV, transmittance, and CA measurements. The as-fabricated ECD displays reversible color changes from colorless to blue meaning the transformation from oxidized state to reduced state upon switching electrical potential. The ECD shows a transmittance modulation of 22% at 800 nm with fast response times of 0.29 s for coloring and 3 s for bleaching and coloration efficiency of 67 cm^2/C. It is highly probable that this configuration of SPE can be helpful to investigate applications in smart windows and other electrochromic devices.

LIST OF ABBREVIATIONS

CA: Chronoamperometry
CE: Coloration efficiency
CC: Chronocoulometry
Ch: Chitosan
CV: Cyclic voltammetry / cyclic voltammogram
ECD: Electrochromic device
EIS: Electrochemical impedance spectroscopy
LiTRIF: Lithium trifluoromethane sulfonate
PC: Propylene carbonate
PEDOT:PSS: poly(3,4-ethylenedioxythiophene): polystyrene sulfonate
PEI: Polyethyleneimine
QSPE: Quasi-solid polymeric electrolyte
SEM-EDS: Scanning electron microscopy-energy dispersive X-ray spectroscopy
SPE: Solid polymer electrolyte

REFERENCES

1. Alves R, Sentanin F, Sabadini RC, Pawlicka A, Silva MM. Green polymer electrolytes of chitosan doped with erbium triflate. Journal of Non-Crystalline Solids. 2018;482:183–191.

2. Eren E, Karaca GY, Koc U, Oksuz L, Oksuz AU. Electrochromic characteristics of radio frequency plasma sputtered WO_3 thin films onto flexible polyethylene terephthalate substrates. Thin Solid Films. 2017; 634: 40–50.

3. Alves R, Sentanin F, Sabadini RC, Pawlicka A, Silva MM. Solid polymer electrolytes based on chitosan and $Dy(CF_3SO_3)_3$ for electrochromic devices. Solid State Ionics. 2017; 310:112–120.

4. Wang W, Guan S, Li M, Zheng J, Xu C. A novel hybrid quasi-solid polymer electrolyte based on porous PVB and modified PEG for electrochromic application. Organic Electronics.2018; 56:268–275.

5. Thakur VK, Ding G, Ma J, Lee PS, Lu X. Hybrid materials and polymer electrolytes for electrochromic device applications. Adv. Mater. 2012;*24*:4071–4096.

6. Alves R, Sentanin F, Sabadini RC, Fernandes M, Zea Bermudez Vd, Pawlicka A, Silva MM. Samarium (III) triflate-doped chitosan electrolyte for solid state electrochromic devices. Electrochimica Acta. 2018; 267: 51-62.

7. Ataalla M, Afify AS, Hassan M, Abdallah M, Milanova M, Aboul-Enein HYA, Mohamed A. Tungsten-based glasses for photochromic, electrochromic, gas sensors, and related applications: A review. Journal of Non-Crystalline Solids. 2018; 491: 43–54.

8. Patel GB, Singh NL, Singh F. Modification of chitosan-based biodegradable polymer by irradiation with MeV ions for electrolyte

applications. Materials Science & Engineering B. 2017;225: 150–159.

9. Eren E, Aslan E, Oksuz AU. The Effect of Anionic Surfactant on the Properties of Polythiophene/Chitosan Composites. Polymer Engineering and Science. 2014; 54(11):2632-2640.

10. Aziz SB, Abidin ZHZ, Arof AK. Influence of silver ion reduction on electrical modulus parameters of solid polymer electrolyte based on chitosan silver triflate electrolyte membrane. eXPRESS Polymer Letters. 2010; 4(5):300–310.

11. Arof AK, Osman Z, Morni NM, Kamarulzaman N, Ibrahim Z A, Muhamad M R, Chitosan-based electrolyte for secondary lithium cells. Journal of Materials Science. 2001; 36 : 791– 793.

12. Leones R, Reis PM, Sabadini RC, Ravaro LP, Silva IDA, Camargo ASS de, Donosco JP, Magon CJ, Esperança JMSS, Pawlicka A, Silva MM. A luminescent europium ionic liquid to improve the performance of chitosan polymer electrolytes. Electrochimica Acta. 2017; 240 : 474–485.

13. Alves R, Sabadini RC, Silva DA, Donoso JP, Magon CJ, Pawlicka A, Silva MM, Binary Ce(III) and Li(I) triflate salt composition for solid polymer electrolytes. Ionics. 2018; 24:2321–2334.

14. Majid SR, Arof AK, Electrical behavior of proton-conducting chitosan-phosphoric acid-based electrolytes. Physica B. 2007; 390: 209–215.

15. Cifarelli A, Parisini A, Berzina T, Iannotta S, Organic memristive element with Chitosan as solid polyelectrolyte. Microelectronic Engineering. 2018; 193: 65–70.

16. Chávez E L, Oviedo-Roa R, Contreras-Pérez G, Martínez-Magadán JM, Castillo-Alvarado FL, Theoretical studies of ionic conductivity of crosslinked chitosan membranes.International Journal of hydrogen energy. 2010; 3 5: 12141-12146.

17. Alves R, Sentanin F, Sabadini RC, Pawlicka A, Silva MM. Influence of cerium triflate and glycerol on electrochemical performance of chitosan electrolytes for electrochromic devices. Electrochimica Acta. 2016; 217: 108–116.

18. Eren E, Karaca GY, Alver C, Oksuz AU. Fast electrochromic response for RF-magnetron sputtered electrospun V_2O_5 mat. European Polymer Journal. 2016; 84: 345–354.

19. Zhang R, Xu X, Fan X, Yang R, Wu T, Zhang C. Application of conducting micelles self-assembled from commercial poly(3,4-ethylenedioxythiophene):poly(styrene sulfonate) and chitosan for electrochemical biosensor. Colloid and Polymer Science. 2018; 296:495–502.

20. Poongodi S, Kumar PS, Mangalaraj D, Ponpandian N, Meena P, Masuda Y, Lee C. Electrodeposition of WO_3 nanostructured thin films for electrochromic and H_2S gas sensor applications. Journal of Alloys and Compounds. 2017; 719:71-81.

21. Tang Q, Li H, Yue Y, Zhang Q, Wang H, Li Y, Chen P, 1-Ethyl-3-methylimidazolium tetrafluoroborate-doped high ionic conductivity gel electrolytes with reduced anodic reaction potentials for electrochromic devices. Materials and Design. 2017; 118: 279–285.

22. Deka J R, Saikia D, Lou G-W, Lin C-H, Fang J, Yang Y-C, Kao H-M, Design, synthesis and characterization of polysiloxane and polyetherdiamine based comb-shaped hybrid solid polymer electrolytes for applications in electrochemical devices. Materials and Design. 2017; 118: 279–285.

23. Puguan J M C, Boton L B, Kim H, Triazole-based ionene exhibiting tunable structure and ionic conductivity obtained via cycloaddition reaction: A new polyelectrolyte for electrochromic devices. Solar Energy Materials and Solar Cells. 2018; 18: 210–218.

24. Ramanavicius A, Genys P, Ramanaviciene A, Electrochemical Impedance Spectroscopy Based Evaluation of 1,10-Phenanthroline-5,6-dione and Glucose Oxidase Modified Graphite Electrode. Electrochimica Acta. 2014; 146: 659–665.

25. Wang J-Y, Wang M-C, Jan D-J. Synthesis of poly(methyl methacrylate)-succinonitrile composite polymer electrolyte and its application for flexible electrochromic devices. Solar Energy Materials & Solar Cells.2017; 160: 476–483.

26. Virbukas D, Sriubas M, Laukaitis G. Structural and electrical study of samarium doped cerium oxide thin films prepared by e-beam evaporation. Solid State Ionics. 2015; 271: 98–102.

27. Leones R, Sabadini R C, Esperança J M S S, Pawlicka A, Silva MM, Effect of storage time on the ionic conductivity of chitosan-solid polymer electrolytes incorporating cyano-based ionic liquids. Electrochimica Acta. 2017;232:22–29.

28. Ge Q., Zhou L., Lian Y.-M., Zhang X., Chen R., Yang W., Metal-phosphide-doped $Li_7P_3S_{11}$ glass-ceramic electrolyte with high ionic conductivity for all-solid-state lithium-sulfur batteries. Electrochemistry Communications. 2018; 97: 100–104.

29. Kim H., Kim Y.-II, Partial nitridation of Li_4SiO_4 and ionic conductivity of $Li_{4.1}SiO_{3.9}N_{0.1}$. Ceramics International. 2018; 44 : 9058–9062.

30. Liu H-M, Saikia D, Wu C-G, Fang J, Kao H-M, Solid polymer electrolytes based on coupling of polyetheramine and organosilane for applications in electrochromic devices. Solid State Ionics . 2017; 303:144–153.

31. Zhu Y, Otley M T, Alamer F A, Kumar A, Zhang X, Mamangun D M D, Li M, Arden B G, Sotzing G A, Electrochromic properties as a function of electrolyte on the performance of electrochromic devices consisting of a single-layer polymer. Organic Electronics. 2014; 15 : 1378–1386.

32. Andrade JR, Raphael E, Pawlicka A. Plasticized pectin-based gel electrolytes. Electrochimica Acta. 2009; 54: 6479–6483.

33. Ledwon P, Andrade JR, Lapkowski M, Pawlicka A. Hydroxypropyl cellulose-based gel electrolyte for electrochromic devices. Electrochimica Acta. 2015; 159:227-233.

34. Liu S, Wang W. Improved electrochromic performances of WO_3-based thin films via addition of CNTs. J Sol-Gel Sci Technol. 2016; 80:480–486.

35. Rocha MD, He Y, Diao X, Rougier A. Influence of cycling temperature on the electrochromic properties of WO3/NiO devices built with various thicknesses. Solar Energy Materials and Solar Cells. 2018; 177: 57–65.

36. Ling H, Liu L, Lee PS, Mandler D, Lu X. Layer-by-Layer Assembly of PEDOT:PSS and WO3 Nanoparticles: Enhanced Electrochromic Coloration Efficiency and Mechanism Studies by Scanning Electrochemical Microscopy. Electrochimica Acta. 2015; 174:57–65.

37. Kadam LD, Patil PS. Studies on electrochromic properties of nickel oxide thin films prepared by spray pyrolysis technique. Solar Energy Materials & Solar Cells. 2001; 69:361-369.

38. Chang-Jian C-W, Cho E-C, Yen S-C, Ho B-C, Lee K-C, Huang J-H, Hsiao Y-S. Facile preparation of WO_3/PEDOT:PSS composite for inkjet printed electrochromic window and its performance for heat shielding. Dyes and Pigments. 2018; 148:465-473.

39. Zhang S, Sun G, He Y, Fu R, Gu Y, Chen S. Preparation, Characterization, and Electrochromic Properties of Nanocellulose-Based Polyaniline Nanocomposite Films. ACS Appl. Mater. Interfaces 2017, 9, 16426−16434.

40. Kalagi S S, Dalavi D S, Mali S S, Inamdar A I, Patil R S, Patil P S, Study of Novel WO_3-PEDOT:PSS Bilayered Thin Film for Electrochromic Applications. Nanoscience and Nanotechnology Letters. 2012;4:1146-1154.

41. Patil DS, Pawar SA, Hwang J, Kim JH, Patil PS, Shşn JC. Silver incorporated PEDOT: PSS for enhanced electrochemical performance. Journal of Industrial and Engineering Chemistry. 2016;42: 113–120.

42. Kawahara J, Ersman PA, Engquist I, Berggren M. Improving the color switch contrast in PEDOT:PSS-based electrochromic displays. Organic Electronics. 2012; 13 :469–474.

43. Assis LMN, Leones R, Kanicki J, Pawlicka A, Silva MM. Prussian blue for electrochromic devices. Journal of Electroanalytical Chemistry. 2016. 777:33–39.

44. Eren E, Alver C, Karaca GY, Uygun E, Oksuz AU. Enhanced electrochromic performance of WO_3 hybrids using polymer plasma hybridization process. Synthetic Metals. 2018; 235: 115–124.

45. Firat YE, Peksoz A, Efficiency enhancement of electrochromic performance in NiO thin film via Cu doping for energy-saving potential. Electrochimica Acta. 2019; 295:645-654.

46. Chen X, Yang M, Qu Q, Zhao Q, Zou W. A regiosymmetric blue-to-transmissive electrochromic polymer based on 3,4-ethylenedioxythiophene with bromomethyl pendant groups. Journal of Electroanalytical Chemistry. 2018; 820 : 60–66.

47. Bathe RB, Patil PS. Electrochromic characteristics of fibrous reticulated WO_3 thin films prepared by pulsed spray pyrolysis technique. Solar Energy Materials & Solar Cells. 2007; 91: 1097–1101.

48. Kiristi M, Bozduman F, Oksuz AU, Oksuz L, Hala A. Solid State Electrochromic Devices of Plasma Modified WO3 Hybrids. Ind. Eng. Chem. Res. 2014; 53: 15917−15922.

49. Fernandes M, Freitas VT, Pereira S, Fortunato E, Ferreira RAS, Carlos LD, Rego R, Bermudez VdZ. Green Li^+-and Er^{3+}-doped poly(ε-caprolactone)/siloxanebiohybrid electrolytes for smart electrochromic windows. Solar Energy Materials & Solar Cells 2014; 123: 203–210.

50. Dulgerbaki C, Oksuz AU. Fabricating polypyrrole/tungsten oxide hybrid based electrochromic devices using different ionic liquids. Polym. Adv. Technol. 2016;27: 73–81.

51. Santos GH, Gavim AAX, Silva RF, Rodrigues PC, Kamikawachi RC, Deus JFd, Macedo AG. Roll-to-roll processed PEDOT:PSS thin films: application in flexible electrochromic devices. J Mater Sci: Mater Electron.2016; 27(10) 11072-11079.